

OVERVIEW OF ALTERNATIVE BUNCHING AND CURRENT-SHAPING TECHNIQUES FOR LOW-ENERGY ELECTRON BEAMS*

Philippe Piot^{1,2}

¹ Department of Physics and Northern Illinois Center for Accelerator & Detector Development, Northern Illinois University, DeKalb, IL 60115, USA

² Accelerator Physics Center, Fermi National Accelerator Laboratory, Batavia, IL 60510, USA

Abstract

Techniques to bunch or shape an electron beam at low energies ($\mathcal{E} < 15$ MeV) have important implications toward the realization of table-top radiation sources or to the design of compact multi-user free-electron lasers. This paper provides an overview of alternative methods recently developed including techniques such as wakefield-based bunching, space-charge-driven microbunching via wave-breaking, ab-initio shaping of the electron-emission process, and phase space exchangers. Practical applications of some of these methods to foreseen free-electron-laser configurations are also briefly discussed.

INTRODUCTION

Schemes to enhance the peak current of electron bunches have a vast range of applications. In radiation processes radiating at a given wavelength λ , electrons within a duration $\tau \leq \lambda/c$ radiate in phase thereby enhancing the radiation flux [1]. Likewise low-energy *short* electron bunches can be injected in short-wavelength accelerators, e.g., based on laser-plasma wakefield [2]. In addition to compression, the capability to tailor the current profile of these electron bunches can also serve further applications, e.g., to produced narrow-band radiation (using a train of short electron bunches) [1], enhance the transformer ratio for beam-driven accelerator (ramped current profiles [3]) or mitigate phase-space dilutions arising from collective effects, e.g., coherent synchrotron radiation [4].

Techniques to alter the current distribution can be casted into four categories: (i) ab-initio tailoring of the emission process, (ii) introduction of energy-position correlation within the bunch with subsequent bunching in longitudinally-dispersive beamline, (iii) the direct shaping of the beam by ab-initio shaping of the bunch at its formation stage, and (iv) phase-space manipulations between two degrees of freedoms to map a transversely tailored distribution onto the current profile.

Throughout this paper we employ the longitudinal phase space (LPS) coordinates (ζ, δ) associated to an electron within the bunch. Here ζ is the axial position with respect to the bunch centre and δ is the fractional momentum spread.

* This work was supported by the US-DOE contract DE-SC0011831 with Northern Illinois University. Fermilab is operated by Fermi Research Alliance, LLC under Contract No. DE-AC02-07CH11359 with the US DOE.

AB INITIO METHODS

Photoemission from Shaped Laser Pulses

Photoemission electron source are widespread in operating and foreseen FEL facilities. The electron bunches produced in this type of sources have, at best, durations comparable to the illuminating laser pulse. However the duration is influenced by space charge and RF effects (in the case of RF guns). Figure 1 illustrates the typically achieved compression for a low (0 nC) and high (1 nC) bunch charge. Some bunch compression can be achieved by phasing the laser closer to zero crossing phase ($\varphi = 0^\circ$ in our convention) to the detriment of the transverse emittance. On another hand employing shorter laser bunch results in operating the source in the "blow-out" regime which leads to a large space-charge-induced bunch lengthening [5–7]. The latter regime of operation leads to linearized longitudinal phase space (LPS) which can be subsequently manipulated to yield very short bunches [5].

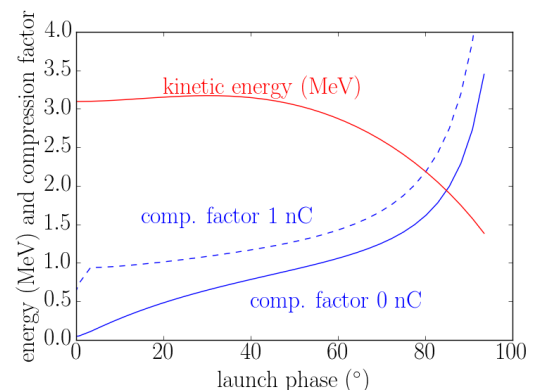


Figure 1: Compression factor (defined as the ratio of the final electron-bunch duration to laser-pulse duration) computed for an L-band RF gun with a 3-ps laser pulse with (dash line) and without (solid trace) accounting for space charge effects.

An interesting area of research is the possibility of tailoring the temporal profile of the emission process. This is particularly attractive in photoemission sources where the emitted electron-bunch distribution initially mirrors the temporal profile of the laser pulse impinging on the cathode. Consequently, laser shaping plays a central role and methods to temporally tailor the laser have been extensively investigated in combination with photo-emission electron sources.

These pulse-shaping techniques include frequency-domain techniques based on spatial-light modulators [8], and DAZZLER systems [9], or simpler time-domain methods using delay lines [10], birefringent crystals [11] or lens with échelon profiles [12]. However these pulse-shaping techniques provide limited ability to form short bunches directly out of an electron source (as pointed out above).

A shape of wide interest is a train of laser pulses to form train of electron bunches. This type of bunches can support the production of coherently enhanced narrowband radiation, or are capable of resonantly exciting a given mode in multi-mode beam-driven accelerating structures. At very low charges, shaping was shown to lead to the formation of electron bunch train [12]. However as the charge increase the density modulation quickly dissipates (it become an energy modulation). Reference [13] pointed out that the information on the initial density modulations is actually imprinted on the LPS and can be eventually recovered after, e.g., after acceleration, using a beamline with the proper longitudinal dispersion R_{56} .

An emerging demand for shaped electron bunches also comes from the mitigation of collective effects. Laser shaping was suggested in Ref. [14] to form electron bunches current profile able pre-compensate for energy spread induced by geometric wakefield in, e.g., accelerating cavities. This capability was recently demonstrated at the FERMI@ELETTRA facility [15] where the "flattening" of the LPS was directly measured.

Finally, an important application of shaped electron beams regards the improvement of the transformer ratio \mathcal{R} in collinear beam-driven acceleration methods [3]. In this class of acceleration methods, a drive bunch excites wakefields which can accelerate a delayed "witness bunch". Maximizing \mathcal{R} – the ratio between minimum decelerating field within the drive bunch with the maximum accelerating field experienced by the witness bunch – can enable longer interaction lengths thereby giving rise to higher energy gain for a given energy depletion of the drive bunch. Symmetric drive-bunch distributions are limited to $\mathcal{R} \leq 2$. A recent proposal for a compact short-wavelength multi-user FEL facility based on multiple beam-driven linacs call for transformer ratio $\mathcal{R} \sim 5$ [16]. Most of the transformer-ratio-enhancing shapes that have been proposed so far exhibit discontinuities and are therefore challenging to experimentally realized [17]. Recent numerical investigations pointed out to a class of smooth current profiles adequate to support beam-driven acceleration with enhanced transformer ratios [18]. Figure 2 depicts a simulated laser shape (from a DAZZLER system) and resulting electron-bunch distribution (green-shaded curve) downstream of a linac with wakefield (blue trace) produced in a DLW; see details in [18].

Optically-assisted Field Emission

The capability of forming spatially and temporally localized electron packets via optically-enhanced field-emission from sharp tips has been demonstrated by several groups [19–21]. In brief field emission is a macroscopic manifestation

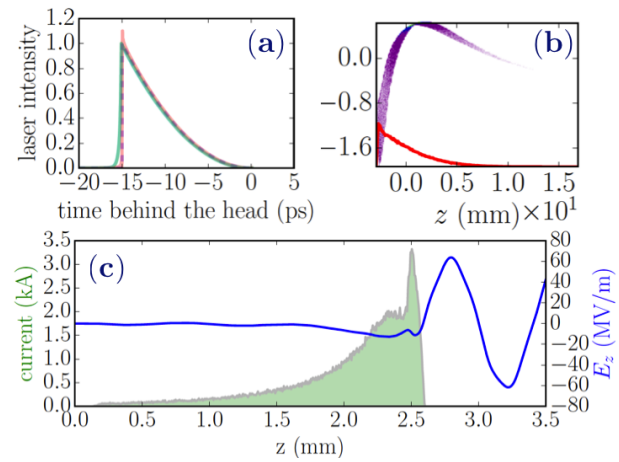


Figure 2: Example of ab-initio temporal shaping of a laser pulse (a) with resulting longitudinal phase space (density plot) and current distribution (red trace) (b) along with final (c) current distribution (green-shaded curve) and excited wakefield in a dielectric accelerator (blue trace). Figure adapted from Ref. [18].

of quantum tunneling, i.e. the "bending" of the potential barrier under the influence of an applied external field. Field emission typically occurs in the presence of high electric field $O(\text{GV/m})$. This field can be locally achieved due to sharp tips or cathode-surface roughness with macroscopic fields on the order of $E \sim 10 \text{ MV/m}$ only. Given the locally-enhanced field $E_e \equiv \beta_e E$, where β_e is the enhancement factor, the field-emitted current density is described by the Fowler-Nordheim (FN) law [22]

$$\mathbf{j} = aE_e^2 \exp\left(-\frac{b}{E_e}\right) \hat{\mathbf{n}}, \quad (1)$$

where $\hat{\mathbf{n}}$ is the normal to the local surface and a and b are positive constants that depend on the material. When the applied field is time dependent i.e. $E(t) = E_0 \cos \omega t$, the field emission is pulsed $\mathbf{j}(t)$ and bunches are formed. In a regime where a high-intensity laser pulse impinges the cathode, the bunch duration is given by the laser period ($\tau \sim 2 \text{ fs}$ for a 800-nm laser pulse).

Figure 3 presents particle-in-cell simulations results of an optically-assisted field emission process from a nanohole using the program WARP [23]. The resulting LPS recorded on a plane 300-nm downstream of the cathode displays modulation with periodicity on the order of 800 nm consistent with the laser wavelength. The noise on this simulation is dominated by the statistics: a single nanohole produces only 200 electrons. Combining several nanoholes in an array [24] would reduce the shot noise and increase the bunching factor at the triggering-laser wavelength. Preserving this imprinted information on the LPS during the downstream acceleration, e.g., in an RF gun, would be crucial to ensure the density modulation can eventually be recovered and further compressed.

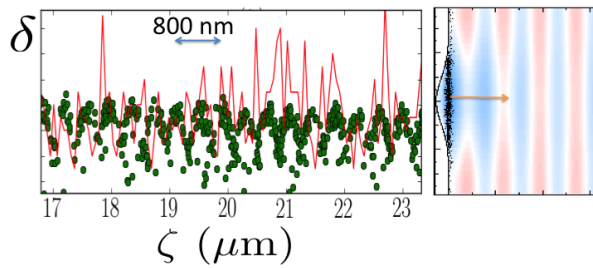


Figure 3: Particle-in-cell simulation of optically-enhanced field emission. Zoomed view (left) of the LPS recorded 300-nm from the cathode surface (the circles represent macroparticle and the red trace is a population histogram) and (right) overview of simulated nanohole geometry. Figure courtesy from A. Lueangarawong (NIU).

This optically-enhanced field-emission technique could in principle be extended by considering a two-dimensional arrays of nanoholes thereby allowing for the generation of electron “crystals” tailored for coherent emission in, e.g., inverse Compton scattering setups.

ENERGY-MODULATIONS TECHNIQUES

Bunching low energy-electron (non-relativistic) beams is often accomplished via the introduction of velocity modulations. This technique was further adapted for higher energy electron beam, e.g., typically produced in photoinjectors using energy-modulation methods to bunch the beam prior to its injection in a downstream linac [25], or to produce ultra-short bunch for, e.g., ultra-fast-electron-diffraction application [5].

Introducing an energy modulation of the form $\delta_0 = \sum_{i=1}^n A_i \cos(k_i \zeta_0 + \phi_i)$ (where A_i , k_i and ϕ_i are respectively the energy-normalized amplitude, wavevector and phase associated to the electromagnetic waves used to introduce the modulation). Given the energy modulation and a downstream beamline with longitudinal dispersion R_{56} , the final electron position within the bunch is $\zeta = \zeta_0 + R_{56} \delta_0$ (linear approximation). Typically the R_{56} is introduced by dispersive beam lines, e.g. chicanes. Here we note that for non ultra-relativistic beam, a drift of length D has a longitudinal dispersion given by $R_{56} = -\frac{D}{\beta^2 \gamma^2}$.

Modulations via Radiation Fields

It has long been recognized that the short-range radiation field or wakefield could be capitalized on to introduce correlation in the LPS. Wakefields have been recently employed to introduce energy modulation or remove remanent time-energy chirps downstream of bunch compressors [26, 27]. The ability of some compact structures, e.g., dielectric-lined waveguides (DLWs), to support high-frequency modes (e.g. in the THz regime) has also enable the impression of energy modulation for possible bunch-train generation [28]. It was recently recognized that the introduced energy modulation is large enough to directly enable bunching in a subsequent

drift when combine with low-energy beams [29]. The interaction of a bunch with its wakefield lead to an energy change described by the convolution integral

$$\Delta \mathcal{E}(\zeta) = LQ \int_{-\infty}^{\zeta} G(\zeta - \zeta') \Lambda(\zeta') d\zeta', \quad (2)$$

where Q is the bunch charge, L the length of the structure, $\Lambda(\zeta)$ is the charge distribution (satisfying $\int \Lambda(\zeta) d\zeta = 1$), and the Green’s function taken to be $G(\zeta) = 2\kappa \cos(k\zeta)$ for a single-mode structure with wavevector k and loss factor κ . In order to illustrate the scheme we consider a parabolic charge-density profile $\Lambda(\zeta) = [3Q/(2a^3)](a^2 - \zeta^2)$ for $|\zeta| \leq a$ where a is the half-width of the distribution; see Fig. 4(a). Figure 4(b) illustrates for two case of mode wavelength. When the rms bunch length fulfills $\sigma_\zeta \approx \lambda/2$; the wakefield introduces a single-cycle energy modulation while in the case $\sigma_\zeta \approx 4\lambda$ the wakefield impresses a few-period energy modulation. The former case yields to an energy depression between the head and tail of the bunch which has the proper sign to be compressed via ballistic bunching in a subsequent drift. Although the introduced chirp is nonlinear, it can eventually lead to the production of a high-peak current for a fraction of the bunch population while the remaining population is debunched. Despite this drawback, this scheme is appealing given its simplicity and absence of need for a precisely synchronized external field as required in, e.g., ballistic bunching based on a buncher cavity [5]. Additionally, for the case of an energy modulation [red trace in Fig. 4(b)], the modulation converts into a density modulation in the drift following the wakefield structure and leads to the generation of a train of bunches as illustrated in Fig. 5. The numerical simulations were carried out for a configuration consisting of an RF gun, a dielectric-lined waveguide (DLW), and two solenoids [29]. Overall the formation of bunch trains with

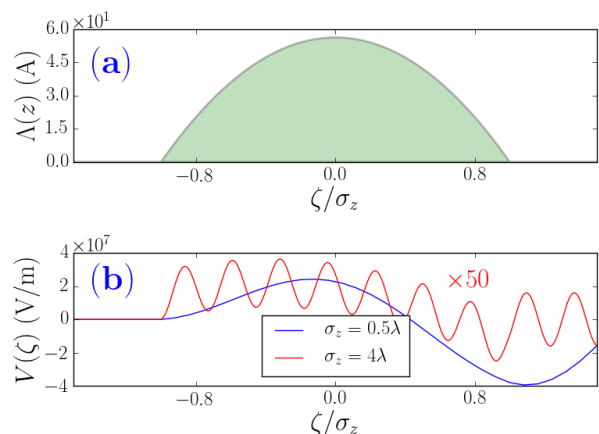


Figure 4: Parabolic charge distributions (a) and corresponding wake potential (b) for two cases of ratio between the rms bunch length σ_ζ and DLW fundamental-mode wavelength λ . The head of the bunch corresponds to $\zeta \leq 0$. The wake potential associated to the $\sigma_\zeta = 4\lambda$ case is scaled by a factor 50 for clarity.

this technique leads to higher peak current and bunching factors than the wave-breaking method discussed in the next section.

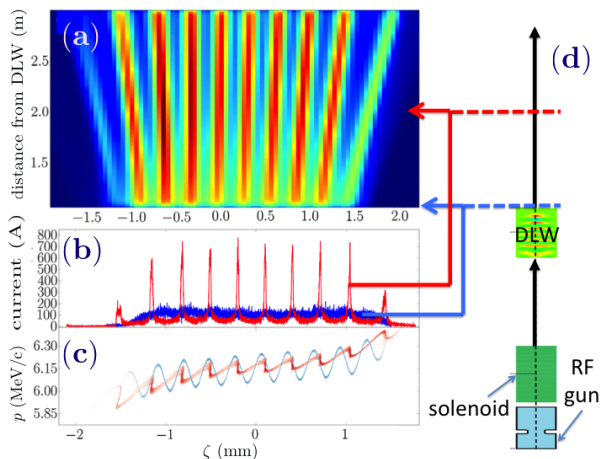


Figure 5: Example of bunch train formation using wakefields. Evolution of the bunch density distribution behind the DLW structure (a) with corresponding initial (blue) and final (red) current (b) and longitudinal phase space (a). The schematic (d) shows the simulated setup. Figure adapted from Ref. [29].

It was also suggested to cascade several DLWs to form ultrashort temporal structures on the bunch in a manner similar to the EEHG technique [30]. The scheme, dubbed wakefield-assisted high-harmonic generation (WAHHG), was simulated using a 5-MeV beam produced in a S-band photoinjector. At these low energies, the chicanes required to introduce the required longitudinal motion can be replaced by drift spaces [31]. Figure 6 demonstrates the concept of WAHHG, the beam evolution is identical to the EEHG method albeit for the reduced number of modulation (given that the bunch length is only one order of magnitude larger than the wavelength of the mode supported by the DLW mode (typically $\lambda \sim 100 \mu\text{m}$). Scaling the technique to shorter wavelength is possible but would require DLWs with smaller apertures with associated impact on the electron beam transmission. The technique was also implemented at higher beam energy using a series of modulator-chicane modules as done for the EEHG approach [32].

Finally, it should be pointed out that other wakefield mechanisms, e.g., the use of a corrugated pipes [3] or plasmas could provide alternatives to DLWs while leading to similar results.

Modulations via Velocity Fields

An interesting and rather counter-intuitive technique for producing comb-like electron distributions consist in exploiting the space-charge forces occurring in beam with initial density modulations Ref. [33]. The idea recognizes that in a modulated cold plasma, plasma oscillations occur (with period T_p) and the density modulation cycles to energy modulation and vice versa every $T_p/4$. When the

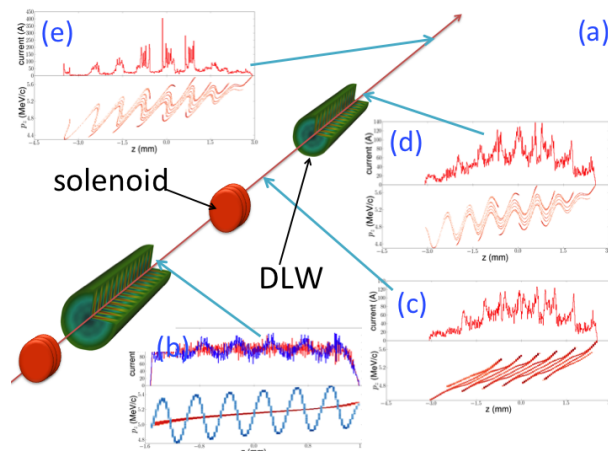


Figure 6: Concept for wakefield assisted high harmonic generation (WAHHG). A modulation is introduced (b) in the first dielectric-lined waveguide (DLW), the subsequent drift over bunch the beam (c) and a final DLW structure superimposes another energy modulation resulting in energy bands (d). After a subsequent drift the energy bands eventually lead to multiple spikes (e). Figure adapted from Ref. [31].

initial modulation becomes large (corresponding to an initial bunching factor $b \approx 1/4$, a phenomenon akin to wave breaking occurs and leads to an enhancement of the bunching factor after $T_p/2$. The technique was experimentally demonstrated at UCLA [33]. Additionally the method was shown to be controllable and capable of forming bunch trains after acceleration in a linac [34].

Modulations via External Fields

Energy modulations can also be introduced via external field as commonly done in conventional setups based on RF components. Here we note that recent progress in the efficient generation of THz pulses have open new possibilities. The THz regime is of interest as the wavelengths $\lambda \in [0.1, 1]$ mm are comparable to the electron bunch lengths typically generated by RF guns. THz radiation generation via optical rectification of an IR laser pulse using a cooled lithium niobate wedged crystal has achieved efficiency on the order of 10% thereby opening the path to mJ THz pulses [35, 36].

A possible configuration for a THz buncher involves an IFEL process [37]. The energy-depleted IR laser pulses used to produce the required UV pulses for photoemission can be directed to an optical-rectification stage to generate $\sim \mu\text{J}$ THz pulses. The produced THz pulse is then co-propagated in an undulator to interact with the electron bunch via an IFEL interaction (coupling through transverse field/velocity). In order to control the phase velocity of the THz pulse, a waveguide is introduced in the undulator. This bunching scheme has the advantage of being immune to jitter as both the bunch and THz pulse are derived from the same laser system. Simulations performed for the PEGASUS photoinjector indicate that the method is well matched to the bunching of ~ 5 MeV electron bunches typically formed in the blow-out

regime and could lead to bunch durations on the order of ~ 10 fs [37].

In the latter THz buncher, the co-propagated THz pulse is a TEM₀₀ mode and the energy exchange occurs through the transverse field. Converting this mode into a radially polarized mode TEM₀₁^{*} (which as an axial electric field) could essentially enable the THz pulse to introduce an energy modulation via coupling through its axial field, e.g., as done in a conventional linac. The challenge resides in the need for mJ pulse compared to the IFEL buncher. In addition, for non ultra-relativistic beams relative phase slippage between the beam and THz pulse becomes important so that the interaction naturally leads to compression via velocity bunching as discussed in [38].

MANIPULATIONS BETWEEN TWO DEGREES OF FREEDOM

Phase-space manipulations within two, or three, degrees of freedom have emerged the past decade [39] and can offer flexible alternative to shape the longitudinal distribution of electron bunches [17]. At low energies these methods can be combined with an interceptive mask, or can directly exploit correlation introduced during the electron-emission process.

In brief the technique rely on exchanging phase-space coordinate between one of the transverse degree of freedoms [here taken to be the transverse phase space (x, x')] with the longitudinal one (ζ, δ) . The main challenge is to devise accelerator beamlines, in the $\bar{X} \equiv (x, x', \zeta, \delta)$ coordinate system, capable of providing a 2×2 anti-block diagonal transverse matrix [14]. Over the years various beamline – or phase-space exchanger beamlines – have been proposed. Most of the exchangers incorporate a deflecting cavity located between either two doglegs [40] or within a chicane [41]. Other schemes include the possible use of transverse-gradient undulators [42].

These techniques were tested at low energies (~ 15 MeV) at the Fermilab’s AOP1 photoinjector [43]. A multi-slit mask

was used to generate a transversely segmented electron bunch which was subsequently transformed into a train of bunch [44, 45]; see Fig. 7. The experiment especially showed the flexibility of the method: varying the input Courant-Snyder parameters upstream of the exchanger beamline could provide control over the bunch train parameters (e.g. separation).

The method was later combined with a transverse shaping of the laser spot on the photocathode and the experiment demonstrated the possibility to map the transverse distribution generated at the cathode surface in the temporal domain; see Fig. 8 [46].

This latter idea was further expanded to combine structured cathodes with nanoscale periodicities to produce trains of bunches at the attosecond scale [47, 48].

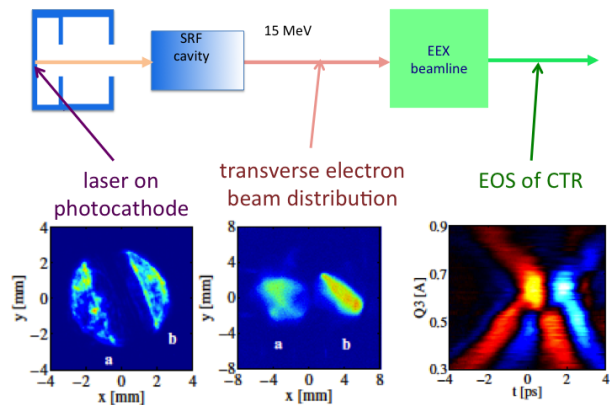


Figure 8: Formation of a two bunch using a transversely segmented photocathode laser pulse via a phase space exchange (top). A twin pulse (to transversely separated laser pulse (lower left image) produces a transversely segmented electron beam (lower middle image) converted into two bunches with variable delay (lower right image). Adapted from Ref. [46].

SUMMARY

This paper provides a non-exhaustive review of concepts recently devised to longitudinally compress or shape the current distribution of non-ultra-relativistic electron bunches.

This paper represents the work of many people and has in particular greatly benefited from collaborations with W. S. Graves (MIT), F. Lemery (CFEL/U. Hamburg), A. Halavanau (NIU), A. Lueangaramwong (NIU), T. Maxwell (SLAC), D. Mihalcea (NIU), and Y.-E Sun (ANL). I am grateful to the FEL15 scientific program committee for the invitation to present this review.

REFERENCES

- [1] A. Gover, Phys. Rev. ST Accel. Beams **8**, 030701 (2005).
- [2] T. Tajima and J. M. Dawson Phys. Rev. Lett. **43**, 267 (1979).
- [3] K. L. F. Bane, P. Chen, P. B. Wilson, SLAC-PUB-3662 (1985).
- [4] C. Mitchell, J. Qiang, and P. Emma, Phys. Rev. ST Accel. Beams **16**, 060703 (2013).

Copyright © 2015 CC-BY-3.0 and by the respective authors

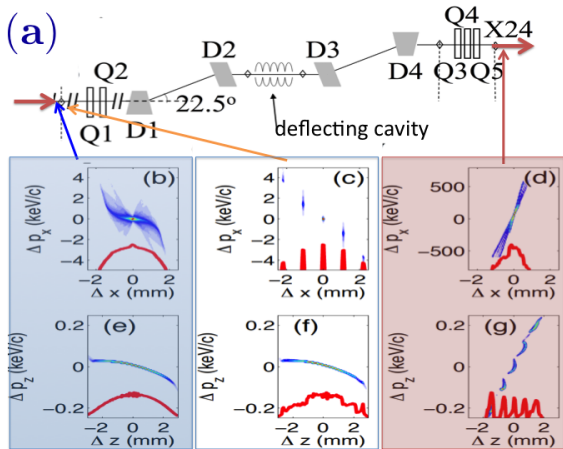


Figure 7: Example of phase space exchanger beam line (a) with corresponding initial (b,e), collimated (c,f) and final (d,g) transverse (b-d) and longitudinal (e-g) phase spaces.

- [5] T. van Oudheusden, P. L. E. M. Pasmans, S. B. van der Geer, M. J. de Loos, M. J. van der Wiel, and O. J. Luiten *Phys. Rev. Lett.* **105**, 264801 (2010).
- [6] P. Musumeci, J. T. Moody, R. J. England, J. B. Rosenzweig, and T. Tran, *Phys. Rev. Lett.* **100**, 244801 (2008).
- [7] P. Piot, Y.-E Sun, T. J. Maxwell, J. Ruan, E. Secchi, J. C. T. Thangaraj, *Phys. Rev. ST Accel. Beams* **16**, 010102 (2013).
- [8] A. M. Weiner, *Rev. Sci. Instrum.*, **71**, 1929 (2000).
- [9] P. Tournois, *Opt. Commun.* **140**, 245 (1997).
- [10] C. W. Siders, J. L. W. Siders, A. J. Taylor, S. Park, and A. M. Weiner, *Appl. Opt.* **37**, 5302 (1998).
- [11] S. Zhou, D. Ouzounov, H. Li, I. Bazarov, B. Dunham, C. Sinclair, and F. W. Wise, *Appl. Opt.* **46**, 8488 (2007).
- [12] Y. Li, K.-J. Kim, *Appl. Phys. Lett.*, **71**, 1929 (2000).
- [13] M. Boscolo, M. Ferrario, I. Boscolo, F. Castelli, S. Cialdi *Nucl. Instrum. Meth. A* **577** 409 (2007).
- [14] M. Cornacchia, S. Di Mitri, G. Penco, and A. A. Zholents, *Phys. Rev. ST Accel. Beams* **9**, 120701 (2006).
- [15] G. Penco, M. Danailov, A. Demidovich, E. Allaria, G. De Ninno, S. Di Mitri, W. M. Fawley, E. Ferrari, L. Giannessi, and M. Trovó, *Phys. Rev. Lett.* **112**, 044801 (2014).
- [16] A. Zholents, W. Gai, R. Limberg, J. G. Power, Y.-E Sun, C. Jing, A. Kanareykin, C. Li, C. X. Tang, D. Yu Shchegolkov, E. I. Simakov, in *Proc. of the 2014 Free-Electron Laser conference (FEL14)*, 993 (2014).
- [17] P. Piot, Y.-E Sun, J. G. Power, and M. Rihaoui, *Phys. Rev. ST Accel. Beams* **14**, 022801 (2011).
- [18] F. Lemery and P. Piot, *Phys. Rev. ST Accel. Beams* **18**, 081301 (2015).
- [19] P. Hommelhoff, C. Kealhofer, M. A. Kasevich, *Phys. Rev. Lett.* **97**, 247402 (2006).
- [20] R. Bormann, M. Gulde, A. Weismann, S.V. Yalunin, and C. Ropers, *Phys. Rev. Lett.* **105**, 147601 (2010).
- [21] M. Krüger, M. Schenk, P. Hommelhoff, *Nature* **475**, 78 (2011).
- [22] R.H. Fowler and L. Nordheim, *Proc. Royal Soc. of London. Series A*, **119**, 173-181 (1928).
- [23] J. L. Vay, D. P. Grote, R. H. Cohen, A. Friedman, *Comput. Sci. Disc.* **5** 014019 (2012).
- [24] R. K. Li, H. To, G. Andonian, J. Feng, A. Polyakov, C. M. Scoby, K. Thompson, W. Wan, H. A. Padmore, P. Musumeci, *Phys. Rev. Lett.* **110**, 074801 (2013).
- [25] G. A. Krafft, in *Proc. of the Microbunches Workshop, AIP Conference Proceedings* **367**, 46 (1996).
- [26] S. Antipov, C. Jing, M. Fedurin, W. Gai, A. Kanareykin, K. Kusche, P. Schoessow, V. Yakimenko, and A. Zholents, *Phys. Rev. Lett.* **108**, 144801 (2012).
- [27] P. Emma, M. Venturini, K. L. F. Bane, G. Stupakov, H.-S. Kang, M. S. Chae, J. Hong, C.-K. Min, H. Yang, T. Ha, W. W. Lee, C. D. Park, S. J. Park, and I. S. Ko, *Phys. Rev. Lett.* **112**, 034801 (2014).
- [28] S. Antipov, M. Babzien, C. Jing, M. Fedurin, W. Gai, A. Kanareykin, K. Kusche, V. Yakimenko, A. Zholents, *Phys. Rev. Lett.* **111**, 134802 (2013).
- [29] F. Lemery, P. Piot, *Phys. Rev. ST Accel. Beams* **17**, 112804 (2014).
- [30] G. Stupakov, *Phys. Rev. Lett.* **102**, 074801 (2009).
- [31] F. Lemery, P. Piot, to appear in *Proc. of the 16th Advanced Accelerator Concept (AAC14) workshop, San Jose CA* (in press, 2015).
- [32] P. Piot, F. Lemery, manuscript in preparation (2015).
- [33] P. Musumeci, R. K. Li, A. Marinelli, *Phys. Rev. Lett.* **106**, 184801 (2011).
- [34] P. Musumeci, R. K. Li, K. G. Roberts, *Phys. Rev. ST Accel. Beams* **16**, 100701 (2013).
- [35] J. Hebling, K.-L. Yeh, M. C. Hoffmann, B. Bartal, K. A. Nelson, *J. Opt. Soc. Am.B* **25**, 6 (2008).
- [36] J. Fülöp, L. Pálfalvi, M. C. Hoffmann, János Hebling, *Opt. Express* **19**, 15090 (2011).
- [37] J. T. Moody, R. K. Li, P. Musumeci, C. M. Scoby, H. To, *AIP Conf. Proc.* **1507**, 722 (2012).
- [38] L. J. Wong, A. Fallahi, F. X. Kärtner, *Opt. Express* **21**, 9793 (2013).
- [39] M. Cornacchia, P. Emma, *Phys. Rev. ST Accel. Beams* **6**, 030702 (2003).
- [40] P. Emma, Z. Huang, K.-J. Kim, P. Piot, *Phys. Rev. ST Accel. Beams* **9**, 100702 (2006).
- [41] D. Xiang and A. Chao, *Phys. Rev. ST Accel. Beams* **14**, 114001 (2011).
- [42] L.D. Duffy, K.A. Bishofberger, B.E. Carlsten, A. Dragt, Q.R. Marksteiner, S.J. Russell, R.D. Ryne, N.A. Yampolsky, *Nucl. Instrum. Meth. Sec. A* **654**, 52 (2011).
- [43] J. Ruan, A. S. Johnson, A. H. Lumpkin, R. Thurman-Keup, H. Edwards, R. P. Fliller, T. W. Koeth, Y.-E Sun, *Phys. Rev. Lett.* **106**, 244801 (2011).
- [44] Y.-E Sun, P. Piot, A. Johnson, A. H. Lumpkin, T. J. Maxwell, J. Ruan, and R. Thurman-Keup, *Phys. Rev. Lett.* **105**, 234801 (2010).
- [45] P. Piot, Y.-E Sun, T. J. Maxwell, J. Ruan, A. H. Lumpkin, M. M. Rihaoui, R. Thurman-Keup, *Appl. Phys. Lett.* **98**, 261501 (2011).
- [46] T. Maxwell, J. Ruan, P. Piot, A. Lumpkin, R. Thurman-Keup, A. Johnson, Y.-E Sun, in *Proc. of IPAC2012, New Orleans LA*, 2789 (2012).
- [47] W. S. Graves, F. X. Kärtner, D. E. Moncton, P. Piot, *Phys. Rev. Lett.* **108**, 263904 (2012)
- [48] E. A. Nanni and W. S. Graves, preprint arXiv:1503.03493 [physics.acc-ph] to appear in *Phys. Rev. ST Accel. Beams* (2015)